2015 ERDKUNDE Vol. 69 · No. 4 · 341–363

WINTER MELT CONDITIONS OF THE INLAND ICE CAP ON KING GEORGE ISLAND, ANTARCTIC PENINSULA

Ulrike Falk and Hernán Sala

With 13 figures, 1 table and 2 photos
Received 23 June 2015 · Accepted 26 November 2015

Summary: The South Shetland Islands are located at the northern tip of the Antarctic Peninsula (AP) which is among the fastest warming regions on Earth. Surface air temperature increases (~3 K in 50 years) are concurrent with retreating glacier fronts, an increase in melt areas, ice surface lowering and rapid break-up and disintegration of ice shelves. We have compiled a unique meteorological dataset for the King George Island (KGI)/Isla 25 de Mayo, the largest of the South Shetland Islands. It comprises high-temporal resolution and spatially distributed observations of surface air temperature, wind directions and wind velocities, glacier ice temperatures in profile with a fully equipped automatic weather station as well as snow accumulation and ablation measurements on the Warszawa Icefield, since November 2010 and ongoing. In combination with long-term synoptic datasets (40 and 10 years, respectively) and atmospheric circulation indices datasets, we have looked at changes in the climatological drivers of the glacial melt processes, and the sensitivity of the inland ice cap with regard to winter melting periods and pressure anomalies. The analysis has revealed a positive trend of 5 K over four decades in minimum surface air temperatures for winter months, clearly exceeding the published annual mean statistics, associated to a negative trend in mean monthly winter sea level pressure. This concurs with a positive trend in the Southern Annular Mode (SAM) index, which gives a measure for the strength and extension of the Antarctic vortex. We connect this trend with a higher frequency of low-pressure systems hitting the South Shetland Islands during austral winter, bringing warm and moist air masses from lower latitudes. A revision of spatial and seasonal changes in adiabatic air temperature lapse rates reveals the high sensitivity of the upper ice cap to free atmospheric flow and synoptic changes. Observed surface air temperature lapse rates show a high variability during winter months (standard deviations up to ±1.0 K/100 m), and a distinct spatial variability reflecting the impact of synoptic weather patterns especially during winter glacial mass accumulation periods. The increased mesocyclonic activity during the winter time in the study area results in intensified advection of warm, moist air with high temperatures and rain, and leads to melt conditions on the ice cap, fixating surface air temperatures to the melting point. This paper assesses the impact of long-term change in large-scale atmospheric circulation and variability and climatic changes on the atmospheric surface layer and glacier mass accumulation of the upper ice cap during winter season for the Warszawa Icefield on KGI. Supplementary data are available at http://dx.doi.org/10.1594/PANGAEA.848704

Zusammenfassung: Die Südshetland-Inseln befinden sich an der nördlichen Spitze der Antarktischen Halbinsel, welche weltweit zu den Regionen zählt, die am stärksten von der globalen Erwärmung betroffen sind. Beträchtliche Änderungen in der Umwelt sind die Konsequenz dieser Erwärmung. Außergewöhnliche Änderungsraten in der bodennahen Lufttemperatur (~3 K in 50 Jahren) gehen einher mit dem Rückzug von Gletscherfronten, der Zunahme von Gletscherschmelze, einem Absenken der Eisoberflächen und der Desintegration von Eisschelfen. Wir haben für die King George Insel/Isla 25 de Mayo (KGI), der größten der Südshetland Inseln, einen einzigartigen Datensatz zusammen getragen. Dieser beinhaltet zeitlich hochaufgelöste und räumliche Messungen von oberflächennaher Lufttemperatur, Windrichtungen und -geschwindigkeiten, Profile von Eistemperaturen mit einer voll ausgestatteten automatischen Wetterstation sowie Messungen von Schnee Akkumulation und Ablation auf dem Warschauer Eisfeld von November 2010 an und andauernd. In Verbindung mit langzeitlichen synoptischen Datensätzen (40 Jahre von 6-stündlichen Messungen) und Datensätzen von atmosphärischen Zirkulations-Indizes, untersuchen wir die klimatologischen Treiber für die Gletscherschmelze-Prozesse und die Vulnerabilität des Inland-Eisschildes mit Schwerpunkt auf den winterlichen Schmelzperioden und Luftdruck-Anomalien. Die Analyse zeigt einen positiven Trend von 5 K über 4 Dekaden in den Tagesminima der Lufttemperatur für die Wintermonate, welche die publizierten Trends der annualen Mittelwerte klar übersteigt, in Verbindung mit einem negativen Trend im monatlichen Mittel des barometrischen Luftdrucks auf Meeresniveau. Diese Änderungen gehen einher mit einem positiven Trend des Southern Annular Mode (SAM) Index, welcher ein Maß für die Stärke und die Ausdehnung des Antarktischen Vortex ist. Wir verbinden diese Beobachtungen mit einer höheren Frequenz von Tiefdruckgebieten, die im Süd-Winter auf die Südshetland-Inseln treffen und warme, feuchte Luftmassen aus den niedrigeren Breiten bringen. Durch seine Exposition ist die Eiskappe von KGI besonders empfindlich gegenüber Änderungen in der winterlichen Akkumulationsperiode von Gletschermassen. Eine Überprüfung der saisonalen und räumlichen Variabilität der Lufttemperaturgradienten zeigen

DOI: 10.3112/erdkunde.2015.04.04 ISSN 0014-0015 http://www.erdkunde.uni-bonn.de

eine höhere Sensitivität des oberen Gletschers gegenüber Zirkulation der freien Atmosphäre und synoptischen Einflüssen insbesondere während der winterlichen Akkumulationsperiode von Gletschermassen. Oberflächennahe Lufttemperaturgradienten zeigen eine hohe Streuung in Wintermonaten (Standardabweichungen bis zu ±1.0 K/100 m) und eine ausgeprägte räumliche Variabilität, welche den Einfluss der synoptischen Wetterphänomene widerspiegelt. Die verstärkte zyklonische Aktivität im Forschungsgebiet in der Winterzeit resultiert in der Advektion feuchter, warmer Luft mit Regen und erhöhten Temperaturen in die Region, so dass sich regelmäßig winterliche Phasen mit Schmelzbedingungen einstellen. In dieser Publikation untersuchen wir den Einfluss von großskaligen und klimatischen Änderungen auf die bodennahe atmosphärische Grenzschicht und in Gletschermassen-Akkumulation des höher gelegenen Eisschildes während der Wintermonate. Die hier publizierten Daten sind verfügbar unter http://dx.doi.org/10.1594/PANGAEA.848704

Keywords: Antarctica, climate change, Southern Annular Mode, adiabatic temperature lapse rate, winter melt

1 Introduction

The Antarctic Peninsula (AP) has a rugged mountain range with a height of up to 2000 m that acts as an orographic barrier to the strong and prevailing westerly winds. It extends furthest north from the central plateau of the Antarctic continent and reaches into the belt of cyclones that encircles Antarctica completely. The AP differs from the rest of the continent by having summer melt seasons that lead to isolated snow- and ice-free areas, which are inhabited by a diverse biota and provides breeding ground for sea mammals and birds.

Over the past decades, the AP has experienced dramatic warming rates. Vaughan et al. (2003) and Cook et al. (2005) report rates of about 2.5 K for the last 50 years, which exceeds several times the global mean warming trend (0.6 K over the past century). This region has thus become a focal point of international scientific research. The cryosphere responds to the higher air temperatures with longer summer melt periods, higher melt rates and an increase in melt areas (Rau and Braun 2002; Vaughan 2006). Hock et al. (2009) estimated the contribution to sea level rise from mountain glaciers and ice shelves surrounding Antarctica to 0.22 ±0.6 mm/a, with a 22 % contribution from the AP. Uncertainties in glacier surface mass balance and mass losses are large (Pritchard and Vaughan 2007; Rignot 2008), but particularly, the estimates for the northern tip of the AP show high spatial variability and considerable uncertainty (Turner et al. 1997; Skvarca et al. 1999; Arigony-Neto et al. 2009). Van den Broeke (2000) observed increases in wind speed and cloudiness, while others report higher precipitation rates (Turner et al. 2004) for the west AP. All these facts are indicators of increased storminess in the region.

The annual course of predominant synoptic weather patterns over KGI is characterized by a higher occurrence of low-pressure systems during the austral summer months, whereas the winter months are dominated by the influence of high pressure systems that originated over the Antarctic plateau. A very important index in this geographical context is the Southern Annular Mode (SAM), also known as the Antarctic Oscillation. Atmospheric circulation in the Southern Hemisphere (SH) is governed by a semiannual oscillation in the strength and extension of the circumpolar low-pressure trough during spring and autumn (van Loon 1967). The SAM-index is defined by Gong and Wang (1999) as the normalized difference in mean sea level pressure (SLP) between 40° and 65°S, whereas Marshall (2003) defines the SAM-index as the monthly mean difference between the mean SLP anomaly at 12 stations evenly distributed close to 45°S and to 65°S. It describes the north-south shift and strength of the westerly wind belt that encircles Antarctica and explains a substantial part of the total variability observed in the extratropical circulation of the SH (Thompson and Solomon 2002). In a satellite-based study for 24 months between July 1991 and January 1995, Lubin et al. (2008) found that the occurrence of mesocyclones at the AP is correlated with the SAM-index and a tendency for positive temperature anomalies in the presence of mesocyclones. In brief, the SAM reflects the atmospheric circulation and the cyclonic activity in the area of the northern AP in a wider sense.

Thompson and Solomon (2002) show that recent trends in the high-latitude SH tropospheric circulation and surface temperatures are consistent with high index polarity of the SAM, and that the observed high latitude changes are characterized by changes in atmospheric circulation. They relate the observed stratospheric ozone depletion over Antarctica with strong stratospheric anomalies in radiation budget, temperature and pressure fields, and the "downward propagation" of the SH circulation anomalies into the troposphere. The variability in SAM accounts for approx. 90 % of the observed cooling at the South Pole and in Eastern Antarctica (Shindell and Schmidt 2004), but for only about 50 % of the observed changes in the AP (Thompson and Solomon 2002). The observed and modelled climatic changes in the troposphere related to SAM occur predominantly during the austral summer and fall, December to May. Gillett et al. (2006) associate a positive SAM-index with a significant warming of the AP in the past five decades, and a significant increase in temperature and precipitation over the land masses in the study area. A positive trend in the SAM index implicates a strengthening of the circumpolar vortex together with an intensification of the westerlies around Antarctica (Marshall 2003). It thus provides an indication of the frequency or occurrence of low-pressure systems hitting KGI, which are the most important drivers of precipitation variability at the northern tip of the AP.

Another prominent driver for climatic change is CO_2 (Solomon et al. 2009). Barrand et al. (2013) found a correlation of melt index and SAM, the El Niño Southern Oscillation and the Southern Oscillation Index (Tedesco and Monaghan 2009; Torinesi et al. 2003; Trusel et al. 2012) to be significant but superimposed by the non-linear response of sea ice in the Bellingshausen sea to the warming of the ocean and the atmosphere (Turner 2004). Clearly, the increase in surface air temperatures at the AP is substantially higher than in the rest of Antarctica and the global mean (Barrand et al. 2013; IPCC 2013), and is accompanied by an increase in precipitation (Turner et al. 1997; van den Broeke et al. 2006) and thus snow accumulation (Thomas et al. 2003). At the same time, ocean temperatures have been rising (Meredith and King 2005), leading to a decrease in sea ice extent (Smith and Stammerjohn 2001). Barrand et al. (2013) found that melt area in the AP derived from QSCAT data (remote sensing scatterometer) to be strongly correlated with October-January averaged SAM-index. We observe consistently higher trends and inter-annual variability during winter months. All literature is focused on the ongoing changes during austral summer. The repeat occurrence of pronounced periods of winter melt is the scope of this paper as is the statistical analysis of uncertainties and errors.

The specific objectives of this paper are: (i) to identify ongoing trends and their relationship with current changes in climate and synoptic circulation for the KGI area, and (ii) to assess spatial and temporal variability of the meteorological drivers in the atmospheric surface layer, with special focus on the austral winter atmospheric surface layer to (iii) draw conclusions on the implications for the glacier mass balance.

2 Study area

KGI is the largest island of the South Shetland Islands, located approx. 120 km from the northwestern coast of the AP. Most of its 1250 km^2 are covered by a temperate ice cap and the non-glaciated areas are composed of nunataks, outcrops, beaches and small stream basins that jointly represent less than 10 % of the total surface (Braun and Hock 2004). The northern coast and the north-facing slopes are relatively regular and gentle, respectively, but on the contrary, southern coast and south-facing slopes are quite irregular and abrupt, respectively (Sala et al. 2014).

According to Rückamp et al. (2011), the highest elevation reaches 720 m a.s.l. in the central ice dome. Nevertheless, secondary peaks of about 500–600 m a.s.l. are frequent throughout the island. The underlying geological structure divides its ice cap into several independent glacial systems (Braun and Hock 2004). The draining glaciers have their terminus on land or are tidewater glaciers; the latter usually do not have floating snouts. Nevertheless, regardless of their terminus characteristics, most of them have had significant retreats in the last few decades, which have been studied by Park et al. (1998), Simões et al. (1999), Braun and Gossmann (2002) and Rückamp et al. (2011), among others. The Warszawa Icefield (WI) covers the southwestern peninsula of KGI and includes two big tidewater glaciers: the Polar Club Glacier and the Fourcade Glacier. The latter drains into Potter Cove (see Photo 1). Our data was mainly obtained on these two glaciers or in the neighboring areas (Fig. 1).

According to Wen et al. (1998) and to Ferron et al. (2001), the near sea level annual average temperature was -2.4 °C and -2.8 °C, respectively during the last decades on KGI. Like the rest of the South Shetland Islands, KGI is under maritime climate conditions. As a consequence, days with positive temperatures are not absent in winter and are frequent in summer. The occurrence of positive temperatures all year round is well-registered as thick and multiple ice lenses even in high elevations of the ice cap. Moderate temperatures during the different seasons of the year are closely associated with the advection

Photo 1: Panoramic view of Potter Cove, King George Island. (Photo: D. López 2012)

of humid and relatively warm marine air masses. The South Shetland Islands, in contrast to the high interior of the West and East Antarctic plateau, are frequently influenced by advection processes that bring warm and moist air masses formed at lower latitudes over the surrounding oceans. Warm advection towards this region is strongly linked with the circumpolar trough of low pressure that is present throughout the year (Parish and Bromwich 2007).

3 Instruments and datasets

3.1 Long-term climate dataset of meteorological observations at Bellingshausen Station

The Russian Bellingshausen Station is located on Fildes Peninsula of KGI at S 62° 12', W 58° 58' at about 14 m a.s.l. The Bellingshausen climate dataset includes 6-hourly measurements of barometric pressure at station level, barometric pressure at sea level, surface air temperature, dew point temperature, relative humidity, total cloud and low cloud, surface wind direction, surface wind speed, precipitation, etc. This time series started in March 1968 and was available until March 2010 (Martianov and Rakusa-Suszszewski 1989; AARI 2014).

It was screened for typing errors, and a quality control analysis was performed marking data as outliers if the distance to the expectation value was more than the six-fold standard deviation.

Figure 2 displays the long-term monthly averages of surface air temperature at Bellingshausen Station, with a 95 % confidence interval with standard errors. The statistics show that air temperatures above the melting point are not unusual even outside of the austral summer (December to February). This analysis is based on the 6-hourly time series for the period March 1968–March 2010. Figure 2 also shows that the long-term monthly averages during summer months are slightly above the melting point. However, the variability is significantly greater in winter than in summer months. The lowest value of the long-term monthly averages is in July with -5 °C. At Bellingshausen Station, the surface air temperature descended well below the standard errors and the minimum can be nearly as low as -30 °C many times during the 40 year time series. But, on the other side, positive air temperatures are not unusual at any month of the year. Furthermore, the above-zero temperatures are within the standard errors of the long-term statistics even during the winter months. June has an exceptionally high standard error on the positive side, meaning a significantly high variability in comparison to other winter months, and also indicating a frequent occurrence of periods with positive air temperatures accompanied with the consequent melt periods. The extreme values are more centered and evenly distributed on both sides of the monthly averages from October to March, indicating that surface air temperature variability is considerably lower during the warmer half of the year.

3.2 SAM-index data derived from NCEP/NCAR Reanalysis 1 dataset

The monthly SAM-index is defined as the difference in the normalized monthly zonal-mean barometric sea level pressure (SLP) between 40°S and 70°S (Nan and Li 2003). The AAO-index as defined by Gong and Wang (1999), is the difference in the

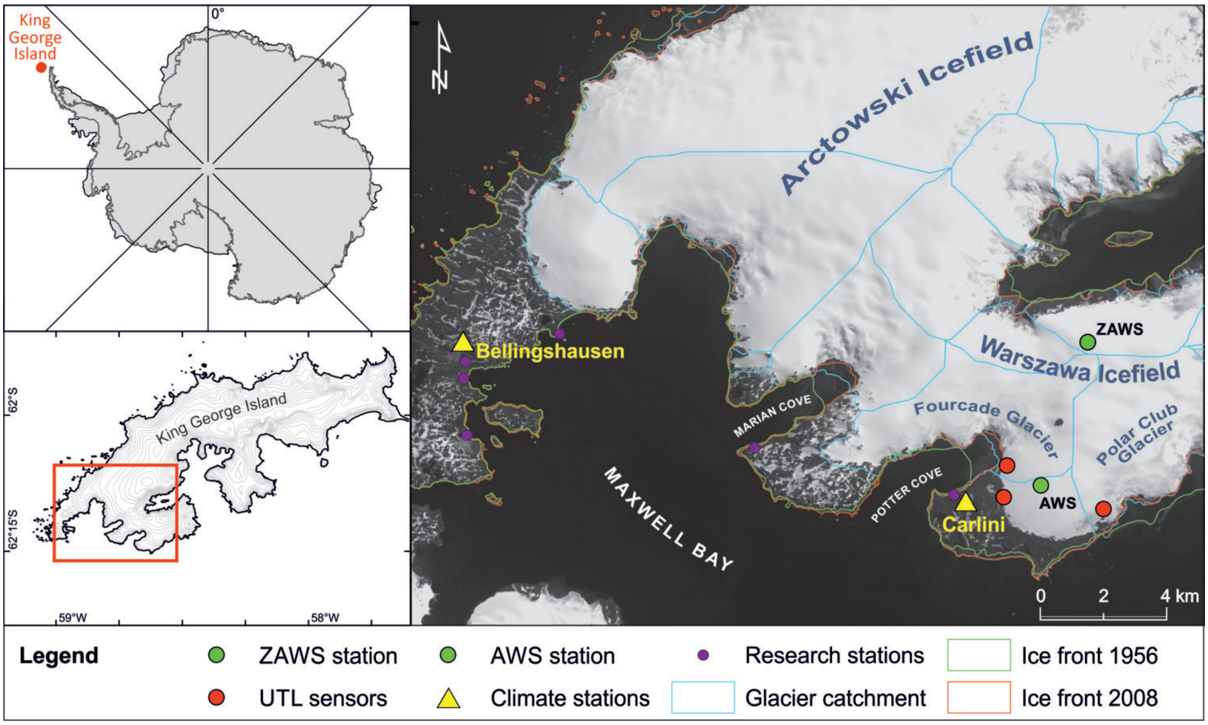

Fig. 1: Map of the study area. Measurements were carried out between November 2011 and March 2013. Background-image: SPOT-4 on 18 November 2010, © ESA TPM, 2010. Ice fronts were calculated by Rückkamp et al. (2011).

normalized zonal-mean SLP between 40°S and 65°S. The SAM-index is a modified AAO-index that uses a slightly different zonal-mean SLP difference, which produces an index that is statistically more robust.

The NCEP/NCAR Reanalysis 1 Project (NNR) performs data assimilation and reanalysis on the basis of multiple sources of datasets from 1948 up to the present (Kalnay et al. 1996). The outputs from the model have different temporal resolutions oriented to different user needs. Long-term monthly means were derived from data of the time period 1981–2010. Marshall (2003) states that the NNR model performance is especially problematic during winter at southern high latitudes, which is probably attributed to sea ice or seasonally different errors in Antarctic surface energy balance. He defines the SAM-index as an observation-based monthly mean difference between the mean SLP anomaly at 12 stations evenly distributed close to 45°S and to 65°S.

The trend analysis of the SAM-index time series from both datasets (Fig. 3) shows a clear positive linear trend towards higher positive values, reflecting a weaker and lesser extension of the Antarctic vortex. Figure 3 shows the average annual SAM-index for the time period 1958–2012, as well as the seasonal variability, defined as the difference between annual maximum and annual minimum of the SAM-index after subtracting the linear trend from the dataset. The observed linear trend in the annual SAM Index over 50 years is equal to "ANN" = 2.03 ± 0.25 (standard error) and is of the same order of magnitude and range as the observed "seasonality". The trend in the SAM index dataset, as derived by Marshall (2009), shows a linear trend of "ANN" = 1.05 ± 0.23. Both SAM index curves are clearly correlated, showing a positive offset of the NNR towards Marshall's SAM index that explains the difference in the linear regression analysis.

Subtracting the linear trend, the general course of annual SAM index can be considered the same for both datasets. A positive SAM-index means a southward contraction of the belt of strong westerly winds that defines the Antarctic vortex, which results in advection of warm moist air in combination with high wind speeds and low pressure along the northwest of the AP. A negative SAM-index reflects an expansion of the Antarctic vortex, thus resulting in a higher impact of the Antarctic high pressure system in the study area at the northern tip of the AP. However, the anomalously strong westerlies instead lead to increased warm advection from the Southern Ocean. The trend towards higher positive values in the SAM index is clearly demonstrated in the long-term dataset (1958–2012).

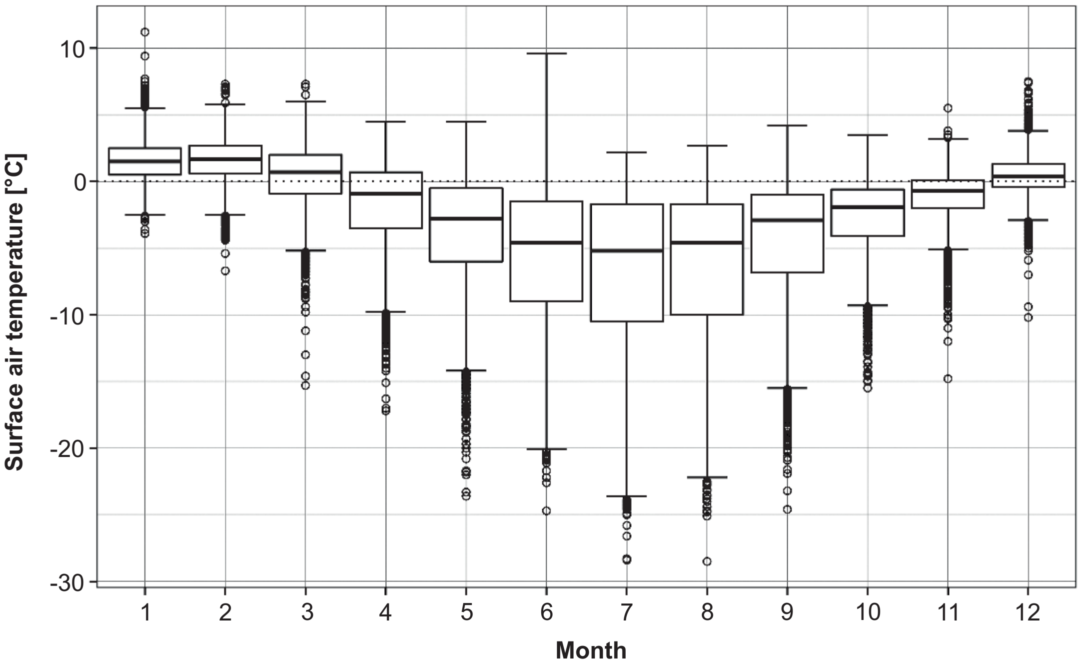

Fig. 2: Monthly statistics of surface air temperature from 6-hourly climate data time series (square: marks the 1st and 3rd quartile, cross bar: shows the median; error bars: standard deviation around mean, circles: outliers) from Bellingshausen Station, KGI, during the period March 1968–March 2010 (Martianov and Rakusa-Suszszewski 1989; AARI 2011)

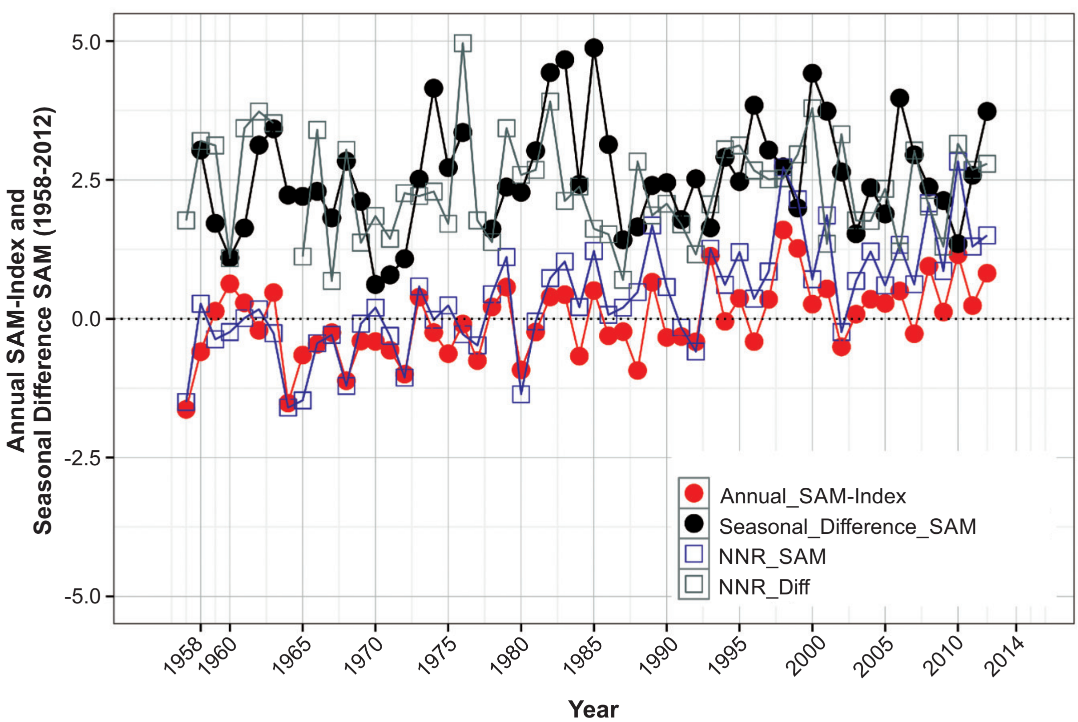

Fig. 3: SAM-index and its seasonal variability, i.e., the difference between maximum and minimum SAM-index of each year, period 1958–2012 from two datasets a) solid dots are the time series from Marshall (2009): the annually averaged SAM index (red), and the intra-annual seasonal difference (black). The open squares denote the data derived from the NNR datasets (Nan and Li 2003; Kalnay et al. 1996): annually averaged SAM index (blue), and intra-annual seasonal difference (grey)

3.3 Long-term climate dataset of meteorological observations at the Argentinean Carlini Station

Carlini Station (formerly Jubany Station, National Meteorological Service of Argentina (SMN)) is located at S 62° 14', W 58° 40' at 15 m a.s.l. We analyzed a climate dataset from this station that contains a 3-hourly time series. This time series is from 01-01-2001 until 01-01-2013 and encompasses measurements of surface air temperature, wind direction and velocity, barometric sea level pressure and cloudiness (SMN 2013). The dataset was screened and flagged using time series statistics analysis; outliers were identified using a six-fold standard deviation approach.

Melt days (MD) were counted as days with daytime air temperatures above 0 °C. Positive degree days (PDD) contain the information on cumulative surface air temperature on melt days, i.e., air temperatures above 0 °C. Remarkable is that during summer, at least one month, often two months, has 30 days with melt conditions. Simple analysis of PDD and MD show that average surface air temperature for melt days is approx. 3 °C at Carlini and approx. 2.5 °C at the glacier station, though a maximum summer value for MD of approx. 10 days is significantly lower than for the observations at the station (Fig. 4).

3.4 Automatic Weather Stations and Temperature Data Logger

In November 2010, we installed an Automatic Weather Station (AWS) at S 62° 14' 09.8", W 58° 36' 48.7" at 230 m a.s.l. on the approximate divide of Fourcade and Polar Club glaciers, which are both part of the Warszawa Icefield (see Photo 2). The AWS is equipped with wind anemometers and vanes (Alpine Wind Monitor), and air temperature and relative humidity sensors (HMP155A) at two heights, five depths of snow and ice temperature measurements (107 Thermistor Probes) installed at depths of 10 m, 5 m, 1 m, and two snow temperature sensors installed at the end of the summer. The AWS includes an NR01, a four-component radiation sensor for up- and down-welling long- and shortwave radiation fluxes, two narrow field infrared temperature sensors IR120 facing northwest and southeast at an angle of 40° to measure surface temperatures, and a SR50A Sonic Ranging Sensor installed at an initial height of 2m to measure surface elevation changes. For data acquisition and storage, a CR3000 Micrologger with extended temperature testing with a 2 GB Compact Flash Card was used. The meteorological sensors were installed on a 3 m tripod that was fixed at poles drilled into the ice. To ensure good quality of radiation measurements, all radiation sensors were

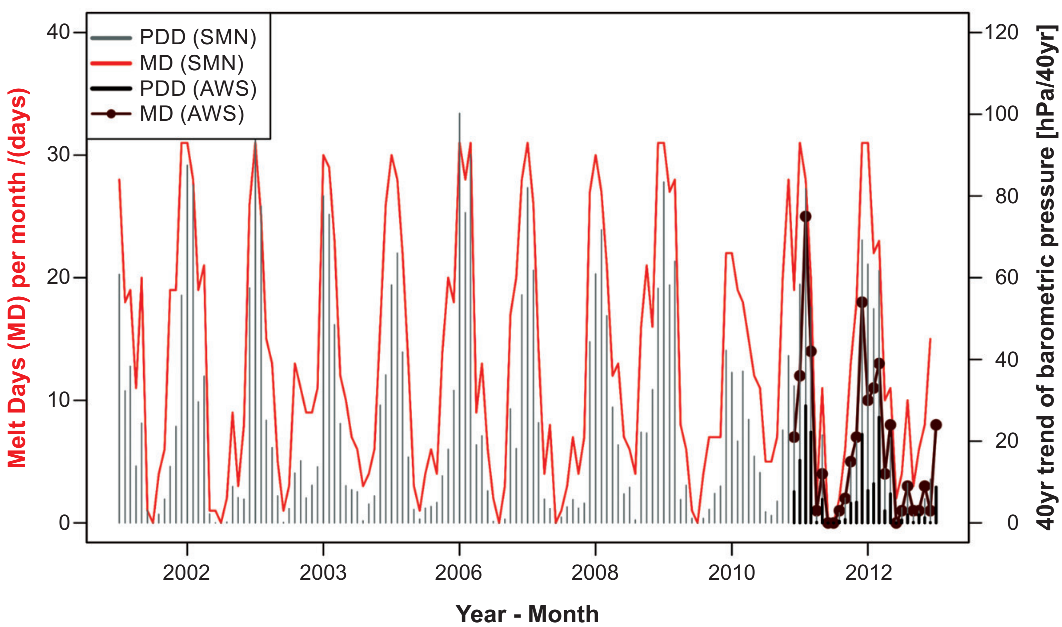

Fig. 4: Positive Degree Days (PDD) and Melt Days (MD) calculated from 3-hourly observations by the National Meteorological Service of Argentina (SMN 2013) at Carlini Station (formerly Jubany Station), KGI. Also plotted are the PDD and MD derived from IMCOAST measurements (black) at AWS (2010-2013)

Photo 2: Automatic Weather Station (AWS) during the accumulation period on the Fourcade Glacier. (Photo: D. López 2012)

mounted on a 3 m boom that extended from the tripod and was fixed to additional 3 m poles drilled into the ice. Levelling and adjustment of sensors were carried out at the beginning and ending of each summer campaign. In particular, at the end of the ablation season, the whole system needed to be lowered about 2 to 3 m due to ablation at the station site. Power supply was realized with solar panels and a battery stack. The measurement rate was set to every 10 seconds with an averaging interval of 10 minutes. In addition to the automated measurements, a mass balance stake was installed at the AWS site. It was measured at the beginning and ending of each summer field campaign in November 2010, February–March 2011, January–March 2012 and during austral winters, starting in 2012 up to May 2015 every 10 to 14 days depending on weather conditions.

In the summer field campaign January–March 2012, an additional Automatic Weather Station denoted ZAWS (see Fig. 1) was installed in the accumulation zone of the WI at S 62° 12' 5.7", W 58° 34' 58.4" and 434 m a.s.l. The ZAWS measured wind speed and direction, air temperature, relative humidity and downward shortwave radiation (by means of Li190SB) for a period of two weeks. All sensors and AWS equipment were purchased from Campbell Scientific, Logan, Utah USA. Three additional air temperature sensors (UTL, Geotest AG, Switzerland) including their respective data loggers were installed relatively close to the AWS site, at different points of the studied glaciers (S 62° 14' 32", W 58° 35' 54", 144 m a.s.l.; S 62° 13' 51" W 58° 38' 05", 65 m a.s.l.; S 62° 13' 58", W 58° 38' 28", 36 m a.s.l.), with the aim to assess the air temperature spatial variability and its adiabatic lapse rates. All temperature sensors were shielded and accuracy is given as ±0.1 °C. The measurements of surface air temperature in the near surface layer above ablation zone of the Fourcade Glacier shows that summertime air temperatures are around 0 °C.

The ice temperature at a depth of 10 m is -1 to -3 °C throughout the year. At 1 m in depth, the ice temperature shows higher variability, probably partly due to air or melt water contact (Fig. 5). After February 2012, the sensor was melted out and showed the surface air temperature and fluctuations. Positive (above 0 °C) air temperature measurements are not unusual during winter time (Fig. 5 above). The data gaps due to power outages during winter do of course add uncertainty to this observation. The power outages during winter 2012, especially in June and July, can be attributed to stormy and overcast conditions with precipitation in form of rain.

The wind direction measurements were corrected for the deviation of the magnetic to true geographic north, with a correction value of 10.7±0.5 degree east derived from calculations of the IGRF12 and WMM2015 model from the NOAA web page (http://www.ngdc.noaa.gov/geomag/declination.shtml).

Figure 6 (left) shows the wind rose for Bellingshausen data (1978–2010), described in

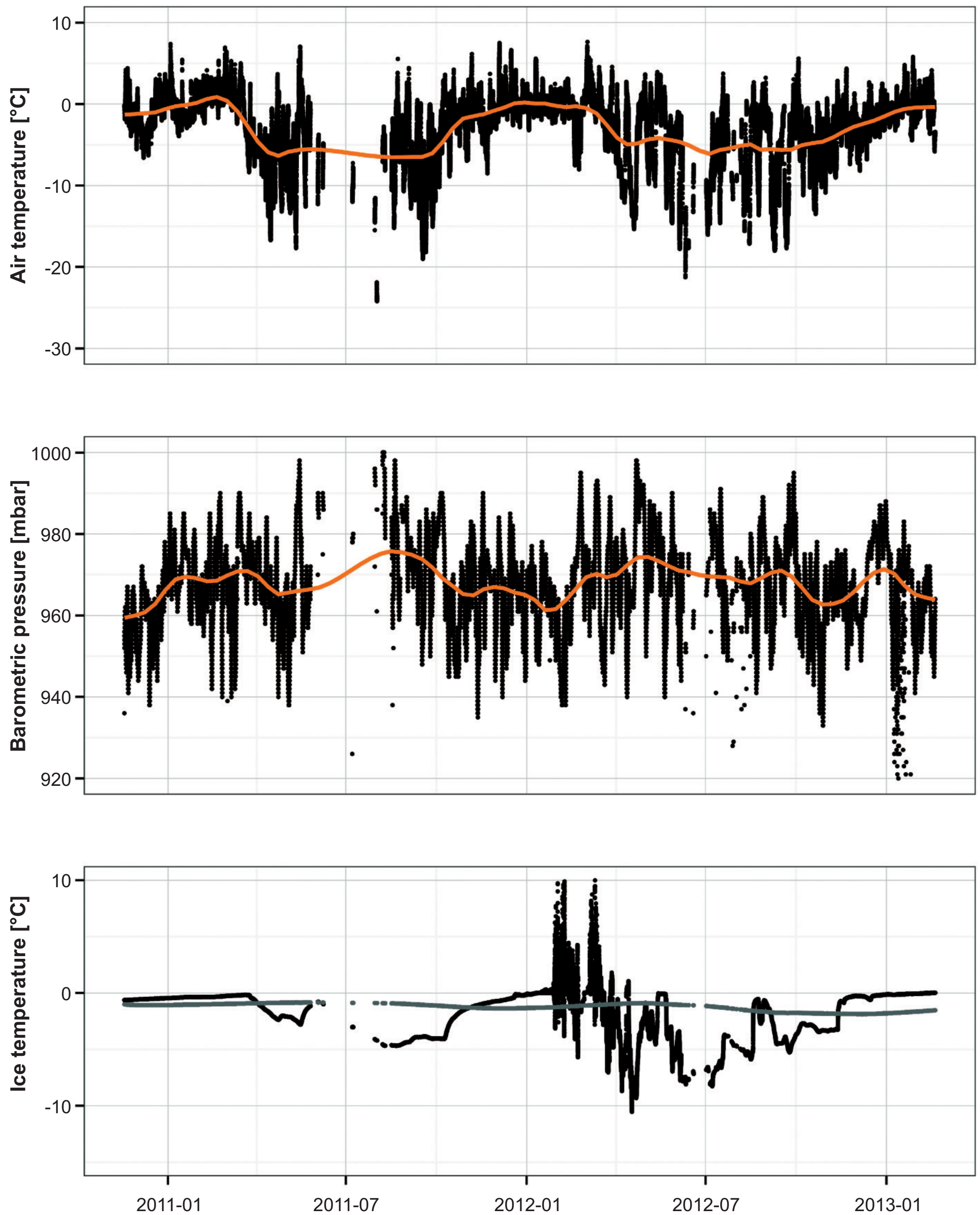

Fig. 5: Meteorological measurements of surface air temperature (2 m), barometric pressure and ice temperatures (black: 30 cm and grey: 10 m depth) at the IMCOAST Automatic Weather Station (AWS) on the Fourcade Glacier, KGI at S 62° 14' 09.8", W 58° 36' 48.7" at 230 m a.s.l.

section 3.1, and (right) the wind rose from the IMCOAST AWS station (Nov 2010 to Feb 2013). A pronounced wind system can be seen for both stations, as well as the impact of the topographic channeling effect. Figure 6 (left) shows of course the long-term wind statistics, whereas the wind rose in figure 6 (right) shows data from two seasons. The datasets do not overlap in time, but due

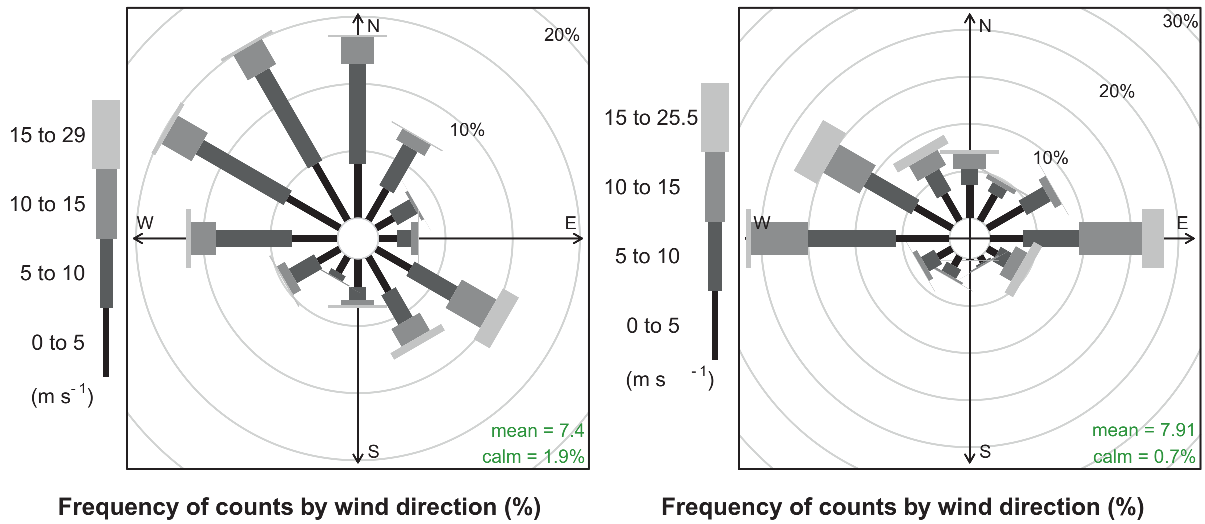

Fig. 6: Meteorological measurements of wind direction and velocity at (left) the Russian Station Bellingshausen (1978–2012) and (right) the IMCOAST Automatic Weather Station (AWS) on the Fourcade Glacier (2010–2013), KGI. Wind velocity counts were clustered into wind direction bins of 30 degree

to the distinct wind system, the 2.5 year statistics are considered representative with an acceptable error. The dominant wind directions differ to about 30 to 45 degrees, and are associated with the topography-induced changes to synoptic conditions. W to N wind directions are associated with the synoptic low pressure systems moving from W to E in front of the western AP and bringing warm and moist air to KGI. E to SE wind directions are associated with cold and dry air winds that are intensified by the katabatic wind system that develops above the inland ice cap of KGI.

Figure 7 shows the prevailing wind directions for each season as measured at the AWS on the Fourcade Glacier. The wind rose is divided into four for the distribution of wind speed and direction for each season: spring (September to November), summer (December to February), autumn (March to May) and winter (June to August). A pronounced seasonal cycle can be seen in the four wind roses. Dominant wind directions during spring and summer are W to NW associated with the synoptic weather patterns, i.e., low pressure systems, bringing warm and moist air from the lower latitudes and E wind directions associated with the prevailing impact of a high pressure system situated on the Eastern side of the AP superimposed by the katabatic wind system. During winter, a higher occurrence of storm events are observed, as well as from NW, i.e., storms bringing rain and positive air temperatures (during June/July 2012).

4 Results

4.1 Long-term climatological time series analysis

A significant warming of annual mean surface air temperature of +2 °C for summer months and +2.4 °C for winter months has occurred in the western AP during the last five decades, as well as an increase of +1.8 °C in the average sea surface temperature over the same period; which has been reported for instance by Rückamp et al. (2011). The study area is of special interest because the surface temperatures are very close to the melting point during summer and winter months. As a consequence, melt events of different spatial and temporal extension can occur year-round.

The trend analysis using weighted linear regression (Fig. 8) shows that minimum temperatures are strongly affected by ongoing change processes. For May and June, an increase in the monthly mean daily minimum air temperature of 4.65±0.9 °C/(40 a), and 3.84±0.8 °C/(40 a) was respectively observed. This relates to a trend in daily mean air temperature per decade of 1.16±0.2 °C decade^{-1} (May) and 0.96±0.2 °C decade^{-1} (June). In August the temperature increase exceeds 5.5±1.0 °C/(40 a), i.e., 1.37±0.3 °C decade^{-1}. The linear trend per decade and season in daily mean air temperature is 0.35 °C decade^{-1} (MAM) and 0.4 °C decade^{-1} (JJA). Zazulie et al. (2010) report comparable but slightly lower values for a linear trend in daily surface air temperature per decade for the Orcadas of 0.29 °C decade^{-1} (MAM) and 0.35 °C decade^{-1} (JJA) for the period 1957–2007, and that the

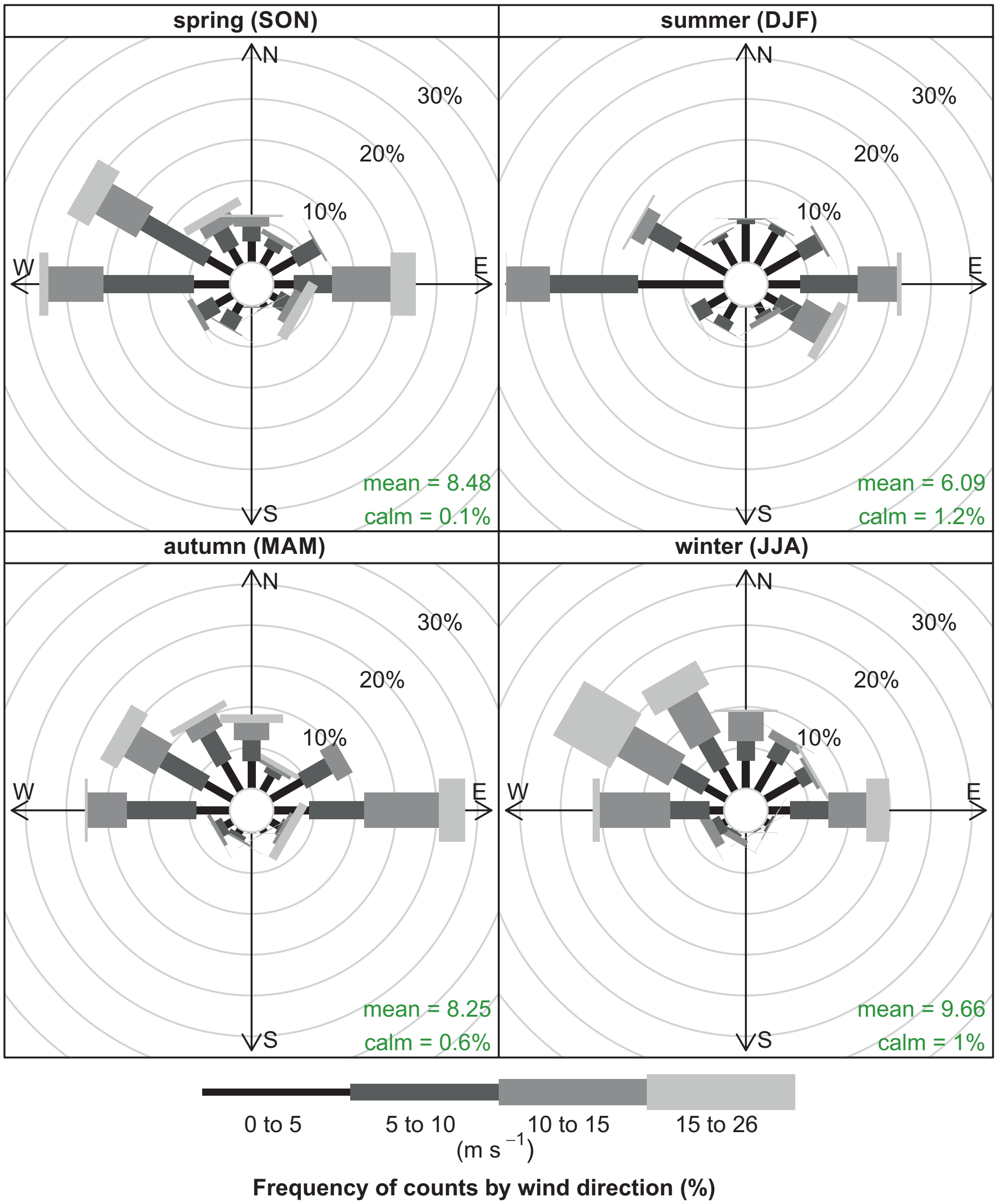

Fig. 7: Meteorological measurements of wind direction and velocity at the IMCOAST Automatic Weather Station (AWS) per season: SON: September-November, DJF: December to February, MAM: March to May, JJA: June to August, on the Fourcade Glacier, King George Island at S 62° 14' 09.8", W 58° 36' 48.7" at 230 m a.s.l.; wind direction bins =30 degree

warming of the cold extremes during austral autumn and winter substantially exceeds that of the average temperatures.

In the monthly average air temperature, the change is greatest during the autumn and early winter months, with a calculated increase over 40 years of 2.4±1.0 °C/(40 a) and as much as 2.6±0.9 °C/(40 a) for May and August, respectively. With regard the monthly mean of daily maximum air temperature, no distinctive behavior can be seen except for a slight cooling trend during winter months and a slight warming trend of 0.7±1.0 ºC/(40 a) in December. The most substantial trends observed during winter months suggest that daily extreme temperatures with very low values are becoming less frequent. The delayed onset of the austral winter reported throughout the literature can be associated with the warming trend clearly observed for the autumn and winter months (April to June and August). During the summer months, the warming trend is not very well-defined; the linear regression analysis even shows a slight cooling trend for December. Regarding the barometric surface pressure, the regression analysis (Fig. 9) yields a negative trend for austral winter months, although the long-term averages show a pronounced seasonal cycle with higher surface pressures during austral winter months.

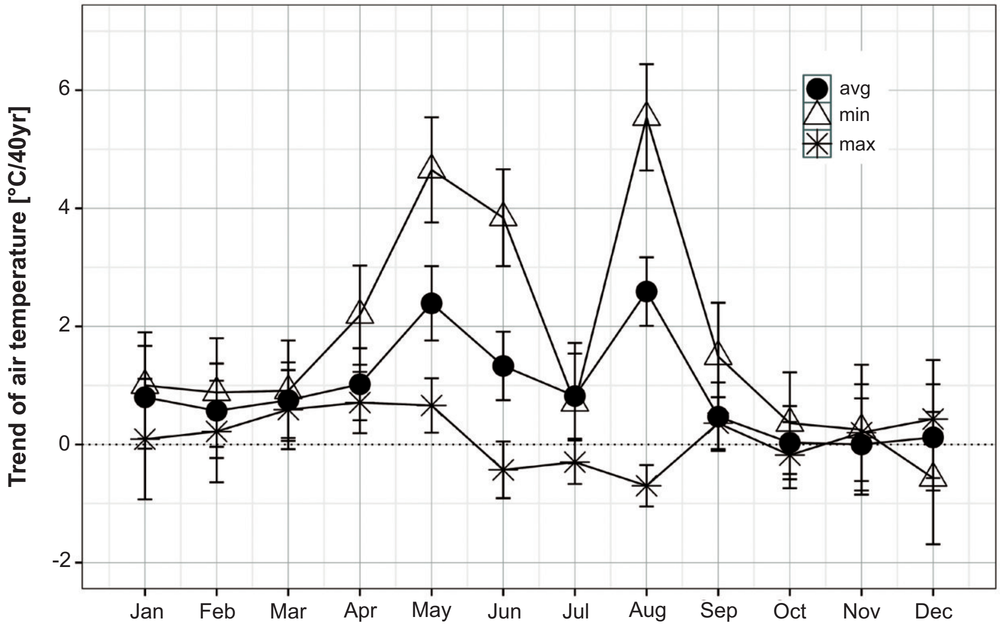

Fig. 8: Trend analysis of monthly averaged (solid dots), monthly minimum (open triangles) and monthly maximum (stars) of surface air temperature at Bellingshausen Station, KGI, during the period September 1968–March 2010 (Martianov and Rakusa-Suszszewski 1989; AARI 2011)

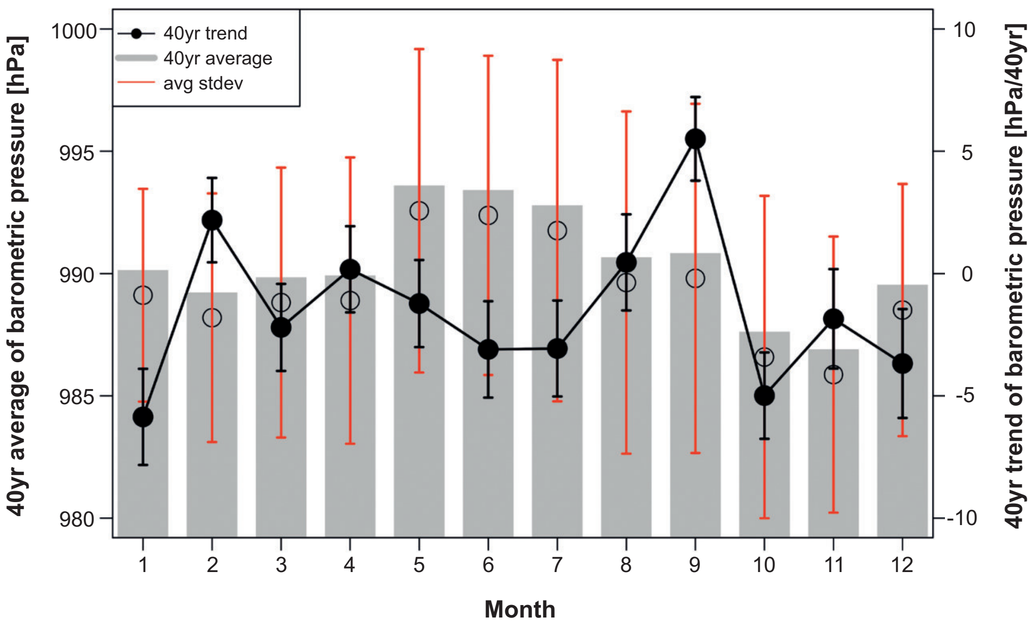

Fig. 9: Trend analysis (black solid dots, right axis) of monthly averaged barometric pressure with standard deviation (black) at Bellingshausen Station, KGI, period Sep 1968–Mar 2010 (Martianov and Rakusa-Suszszewski 1989; AARI 2011). Grey bars are monthly mean values of barometric pressure averaged over 40 years (open circles, left axis) with standard deviation (red)

This suggests a higher exposure to low-pressure systems indicating a change, which is confirmed with the trend analysis of the SAM-index time series, (Fig. 3) towards higher positive values, reflecting a weaker and lesser extension of the Antarctic vortex especially during winter months. For the months October to January, a negative trend in barometric pressure is observed, suggesting a higher occurrence of synoptic lows.

The analysis of covariance maximization (Fig. 10) shows a maximum covariance between surface air temperature in the Bellingshausen dataset and the SAM-index time series at a time lag =0. This last value also supports the existence of a clear correlation between the two time series. A clear correlation between the two variables in the range <15 days shows the predominance of the synoptic systems. Further dominant scales are at about three, six and seven months. At a scale of about nine months, the two data time series become anti-correlated. These scales reflect the seasonal change.

4.2 Spatial variability of surface wind, surface air temperature and lapse rate

Because the study area is located right at the edge of the Antarctic vortex, it may remain within or just outside the vortex depending on the seasonal and inter-annual variability. Generally, during austral winters, the vortex becomes stronger and its extent expands, allowing it to reach lower latitudes. In this way, the South Shetland Islands remain under the influence of the Antarctic high pressure system, receiving cold and dry air masses from the Antarctic plateau. During the austral summer months, KGI is at the edge or simply outside of the Antarctic vortex. As a consequence, during this season, the predominant wind directions are from W to NW, bringing warm and moist air masses from mid latitude oceanic surfaces.

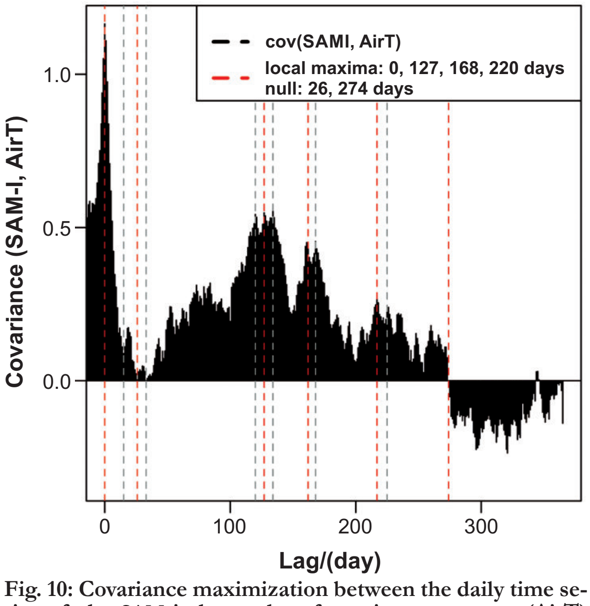

Fig. 10: Covariance maximization between the daily time series of the SAM-index and surface air temperature (AirT) from Bellingshausen Station, KGI, (Martianov and Rakusa-Suszszewski 1989; AARI 2011)

A wind rose showing the statistics of wind direction measurements is given in figure 7. Wind direction and intensity are the 10-min averages of 0.1 Hz measurements at the AWS during the period November 2010 to March 2013. The 10-min averages were clustered into 30° wind direction bins. Highest frequency occurrence of the 10-min values is in the bins from 255–315°, which is associated with transient low-pressure systems.

Most counts of the highest wind velocity 10-min averages, i.e., wind speeds in the range 15 -25.5 m/s, are found in the neighboring 255–285° bin with their predominant occurrence during the summer season. The katabatic wind signal and the influence of the Antarctic high pressure system can be seen in the secondary wind signal with the highest count frequency in the 85–105° bin indicating a strong channeling effect of the ice cap topography showing the superimposition of katabatic winds.

The analysis performed on the datasets from the AWS, the additional automatic weather station placed on the accumulation zone (ZAWS) and the UTL temperature data loggers distributed on the glacier surface, showed that the surface air temperature lapse rate is highly variable and also luv- and lee-side effects of the predominant winds can be deducted from the data (Fig. 11). The adiabatic lapse rate Γ is defined as the differential of surface temperature T to elevation z:

$$-\Gamma = \frac{dT}{dz} \approx \frac{\Delta T}{\Delta z}$$

With regard to the two main wind directions, spatial variability of surface air temperature is expected to differ significantly according to the dominating synoptic systems. Easterly winds bring cold and dry air from the northern-most tip of the AP and Sea Weddell region, with slight foehn and topographic channeling effect due to the Warszawa Icefield that needs to be transversed and the geometry of the Potter Cove (see Photo 1). The westerlies bringing moist and warm air are associated with positive adiabatic lapse rates.

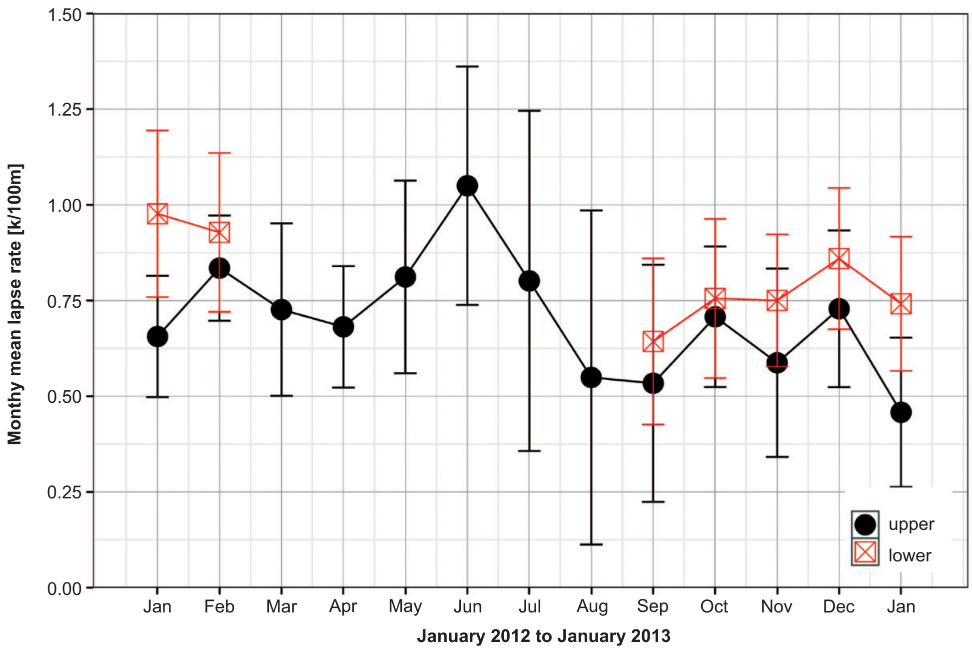

Fig. 11: Monthly mean air temperature lapse rates Γ with standard deviations between a) the AWS (230.5 m) in the glacier ablation zone and the ZAWS and UTL temperature sensor (434.5 m) in the accumulation zone at the upper part of the glacier (solid dots); b) the AWS and a UTL temperature sensor (97.7 m) installed on the southeast-facing slope of the glacier for the time period January 2012–January 2013

The adiabatic temperature lapse rate as defined by the US standard atmosphere is Γ= 0.65 K/100 m and describes a reduction of 0.65 K per 100 m increase in height in the lower troposphere (NOAA 1976). The difference in the calculated surface air temperature lapse rate between the upper transect in the accumulation zone and the lower transect in the ablation zone of the Fourcade Glacier shows a substantial decrease for summer months, in especially for January. Significantly lower lapse rates can be found for the upper glacier. In the austral winter, a lapse rate of Γ > 1 K/100 m (June 2012) is observed, whereas during the austral summer, lapse rates can drop below 0.5K/100m (January 2013).

Figure 12 shows the calculated lapse rate Γ between the AWS (230 m a.s.l.) and the meteorological observations taken by the National Meteorological Service of Argentina (SMN 2013) at Carlini Station (15 m a.s.l.). During the austral summer months, the calculated surface air temperature lapse rate shows a nearly constant value of 1 K/100 m with standard deviations of σ < 0.4 K/100 m. During the winter months, though, it shows a significant decrease of the calculated temperature lapse rate as well as an increase of its standard deviation. In especially during the winter month June 2011, the drop to a negative lapse rate coincides with a significant increase of barometric surface pressure, which shows the influence of the Antarctic high pressure system. Under very stable conditions, the air temperature increases upwards, meaning a winter temperature inversion, a common atmospheric boundary layer condition for snow and ice surfaces (Singh et al. 2011). In June 2012, the value for the calculated lapse rate stays positive, but with a significant increase in the standard deviation and coincides with a significantly low value for the monthly averaged value for barometric pressure, indicating cyclonic activity.

The difference in surface air temperature between the AWS and Carlini Station (SMN) can be as much as 10 °C. According to findings of Braithwaite (1981) and Hock (2003), the PDD is strongly related to glacier melt. Using the moist adiabatic lapse rate of free air, Γ = 0.65 K/100 m (Glover 1999; Thomas et al. 2003; Bassford et al. 2006a,b; de Woul et al. 2006; Raper and Braithwaite 2006), to model the PDD values for the AWS location from SMN data yields a linear regression between modelled and observed values:

$$PDD_{AWS,\,modelled} = 2.73 \times PDD_{AWS,\,observed} + 4.21\,,\ R^2 = 0.84,$$

which shows a clear overestimation of the PDD at the AWS site using the standard adiabatic lapse rate Γ.

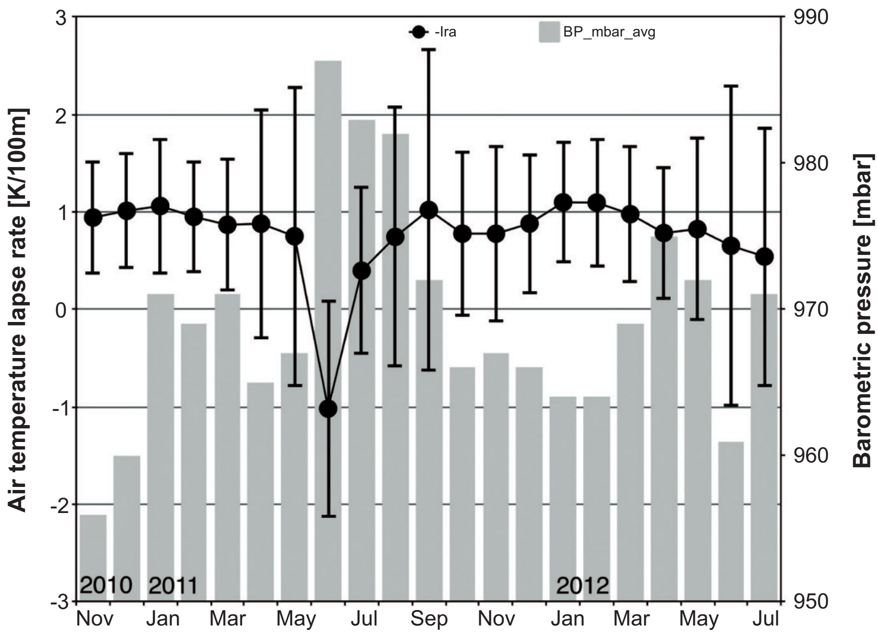

Fig. 12: Monthly mean surface air temperature lapse rate Γ (lra) with standard deviation and barometric pressure (BP_mbar_avg) between the AWS and the Carlini Station for the period November 2010–July 2012 (SMN 2013, and data for the time period until July 2012 from personal communication).

The analysis of surface air temperature lapse rate from the AWS to the upper part of the glacier (Fig. 11) gives a partially contrary behavior with higher lapse rate values during austral winters and the peak value for the month June 2012. The analysis also shows significantly higher standard deviations for months June to August. To assess the spatial variability influenced by exposure of the glacier surface to either the southeast (Antarctic high pressure system) or the northwest (cyclonic activity), an additional UTL temperature sensor was installed on the south-facing slope of the Polar Club Glacier, facing the Bransfield Strait and therefore in full exposure to eastern winds from the Weddell Sea region.

Unfortunately, the measurements stopped after February 2012 and could not be re-initiated before September 2012, so that no data is available for the winter months. Estimates of temperature lapse rates for January 2012 and 2013 show a clear difference of > 0.25 K/100 m to the lapse rate calculated for the Potter Cove slope. There is also a contrary behavior of the two curves for January to February 2012, whereas for the months September 2012 to January 2013, the pattern of the two curves are similar though there is a clear difference in the average monthly values.

The lapse rate calculations show higher variability for surface air temperatures close to 0 °C. Plotting the lapse rate Γ versus wind direction shows that negative values of the lapse rate occur mostly for the 75–105° bin and are otherwise quite randomly distributed. Unfortunately wind direction measurements at the top of the Warszawa Icefield, namely at the ZAWS station, are not available due to sensor malfunction. The lapse rate calculations show a higher variability for lower wind speeds, in especially for wind speeds lower than 5 m/s. This can of course, be associated with ventilation problems of the temperature sensors, but may also indicate a well-mixed atmospheric surface layer of the upper and the lower part of the glacier. There seems to be a wind channeling effect at the lower part of the glaciers (Fourcade and Polar Club) and wind directions do not relate at times (see summer measurements). In particular during the winter time, the air temperature lapse rate shows high variability and takes on values as high as 4.3 °C and as low as -3.3 °C, indicating either strong stable stratification of the atmospheric surface layer and/or a decoupling of the atmospheric surface layer above the higher from the lower part of the Fourcade and Polar Club glaciers. These facts can be interpreted as the higher part of the ice cap being directly exposed to synoptic weather patterns whereas the lower part experiences sheltering effects provided by the Potter Cove. The scattering of temperature lapse rate values is substantially higher during the winter months June–September. The absolute value of mean monthly average of temperature lapse rate is lowest in June for the winter months. Interestingly, the lapse rate recorded during the austral winter month June in 2011 and 2012 show two different synoptic boundary conditions. The high average barometric pressure in June 2011 shows the impact of the Antarctic high pressure system on the research area, together with strong stable stratification and cold air pool in the sheltered Potter Cove. The low barometric pressure in June 2012 implicates cyclonic activity, and the scientific overwinterer at Carlini station reported a dominant storm system with winds from NW over a two-week period (Lopez, personal communication).

The surface air temperature observations and temperature lapse rates estimates are crucial to most glacier melt models and thus for glacier mass balance estimates. The above analysis shows that observations from the ice cap are obligatory for modeling efforts of glacier mass balances and melt rates for the AP.

4.3 Winter melt rates and glacier mass balance

Snow accumulation and ablation was measured using a mass balance stake at the AWS site on the Fourcade glacier. Figure 13 displays the observed snow accumulation and ablation (below), the calculated melt rates (middle), and the surface air temperature measurements (above) at the AWS site. Although the running mean in the air temperature observations is below zero for winter time, the actual 10-min averages show regularly values above the melting point. In austral summer 2011/2012, the mass balance stake had to be exchanged, and unfortunately, in subsequent data analysis, the two time series could not be joined.

The mass balance stake time series show the length of the stake in cm relative to the initial height above the snow surface. Winter melt rates are derived from mass balance stake and snow density measurements and are shown in m water equiv-

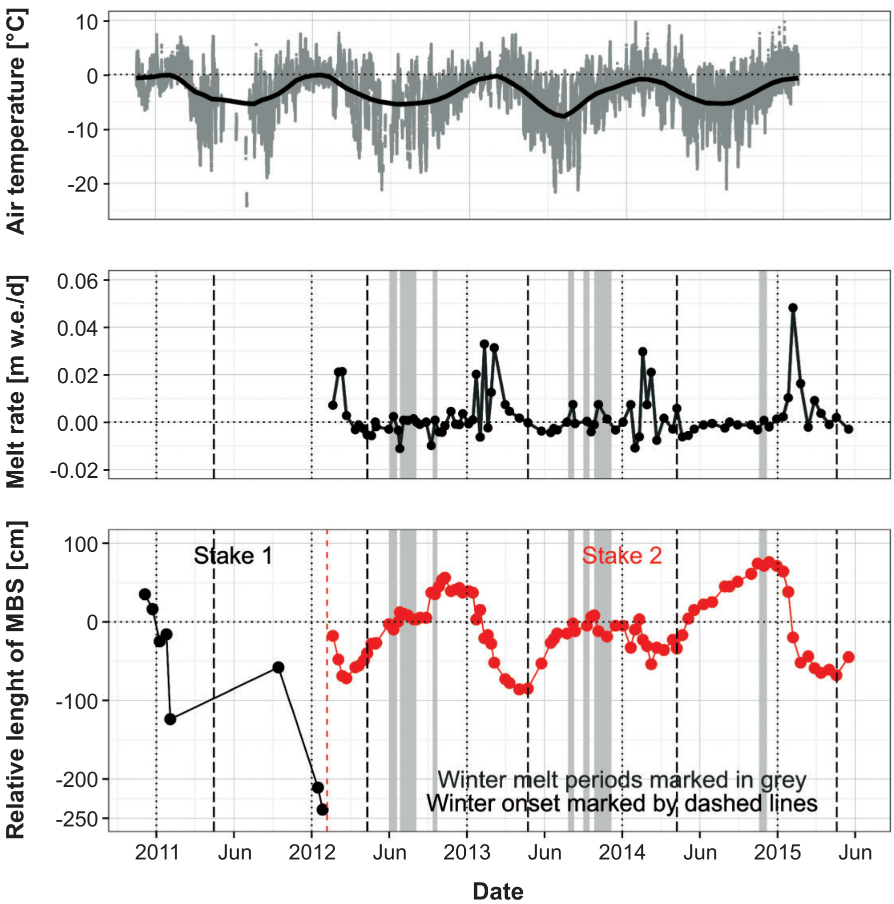

Fig. 13: Air temperature (above) and mass balance stake measurements (below) and calculated melt rates (middle) at the AWS location in the ablation zone of the glacier for the observation time period Nov 2010 to May 2015

alent per day (=m w.e./d). Winter melt periods with positive melt rates are highlighted in the graph by grey shading. It becomes obvious that melt periods occur in all observed austral winters for the period 2012–2015. The austral winter 2013 was the coldest year with the lowest running mean of air temperature measurements and several melt periods. The winter 2014 shows the highest snow accumulation but also then a two-week period with melt conditions could be recorded. An important process seems to be not only snow melt due to positive air temperatures but also snow erosion by precipitation in form of rain, which explains a part of the very high observed melt rates in the austral summer of nearly 50 cm w.e./d. The glacier summer balance b_s is defined as:

$$b_s = \varrho_w D_w - \varrho_s (D_w - (H_s - H_w))$$

where D is the snow depth, H_s and H_w are the stake measurements, and ϱ is the density of firn or ice measured conjointly with the mass balance stakes (Cuffey and Patterson 2010). The indices $i=s,w$ stand for summer and winter respectively.

Table 1 shows the results of summer balance calculations for the time period 2010–2015. Since the mass balance stake time series of the two consecutive stakes could not be joined, the summer balance of the austral summer 2011/2012 is missing. The results show persistently negative values of b_s clearly showing that the location of the AWS is within the ablation zone of the glacier. Falk et al. (2015) derive a firn line position from radar remote sensing of 220m elevation, which is slightly lower than the AWS position at 230 m elevation. The summer balance of 2013/2014 shows a very low absolute value attributed to the cold summer with snow accumulation periods during January and February 2014.

Tab. 1: Glacier summer balance estimates from mass balance stake measurements at the AWS site on the Fourcade glacier, KGI (time period: 2010–2015)

Year of austral summer	Summer balance [m w.e.]
2010/2011	-1.34
2011/2012	–
2012/2013	-2.01
2013/2014	-0.97
2014/2015	-1.96

5 Discussion and conclusions

5.1 Long-term climatic change

The IPCC (2013) predicts increasing surface air temperatures for the AP, exceeding any rate predicted for the rest of Antarctica and the global mean values. This is accompanied by rising ocean temperatures (Meredith and King 2005), increasing amounts of precipitation along the West AP (Turner et al. 1997; van den Broeke et al. 2006) and snow accumulation (Thomas et al. 2003), and a decrease in seasonal sea ice extent (Smith and Stammerjohn 2001). Thompson and Solomon (2002) relate the depletion of stratospheric ozone to the strong anomalies in radiation budget, temperature and pressure fields. They show a "downward propagation" of the stratospheric anomalies into the troposphere to the Southern Hemisphere atmospheric circulation and a positive high-index polarity of the SAM. This results in anomalous strong westerlies and increased advection of warm and moist air from the Southern Ocean to the northern tip of the AP (Gillet et al. 2006).

The long-term air temperature time series at Bellingshausen shows the highest variability in the monthly statistics of 40 year averages of surface air temperatures during the austral winter month June. During this month, positive values of nearly 10 °C lie within the 40 year standard deviation (Fig. 2). The highest monthly trends in air temperature rise can be observed in the monthly minimum and average values for the months May, June, and August (Fig. 8). Although Thompson and Solomon (2002) report the greatest correlation of observed changes for December to May, according to Shindell and Schmidt (2004), the variability in SAM accounts for 90 % of the change observed in Eastern Antarctica, but for only about 50 % of the observed changes in the AP (Thompson and Solomon 2002). Changes in summer months' atmospheric surface layer regime are documented in recent literature (e.g., Barrand et al. 2013), and as the main ablation period length is most important for melt estimates, but changes and trends during the winter time as reported here are significantly higher. The SAM index shows a clear linear trend over the time period 1948 to 2012. The variability of the high index polarity in the SAM index is of the same range as the annual seasonal variability, indicating that the long-term change is of the same order of magnitude as the annual seasonal cycle (Fig. 3). Our analysis of recent and long-term datasets shows an extended autumn and an increasing occurrence of melt periods especially for the winter month June accompanied by advective synoptic patterns bringing warm and moist air from the lower latitudes. A covariance analysis between surface air temperature and SAM (Fig. 10) index shows a high positive correlation for time periods below 20 days representing the length scale of predominant synoptic weather patterns. The local maxima at 4 and 7 months are related to seasonal cycle and length of the ablation period. At a lag of 9 months, the two time series become anti-correlated indicating the seasonal interconnection between the years.

The impact of the ongoing changes in SH atmospheric circulation on the atmospheric surface layer above the inland ice cap of KGI with regard to spatial variability and seasonal patterns are discussed in the following section.

5.2 Air temperature lapse rates in the atmospheric surface layer above the glacier

Due to its maritime position and exposition, KGI is very susceptible to climate change and predominant synoptic systems. The distinct wind regimes lead to a significant spatial variability in the meteorological parameters describing the atmospheric surface boundary layer, one of the most prominent being the adiabatic temperature lapse rate Γ. Braun and Hock (2004) observe temperature lapse rates on the icefield near Bellingshausen Dome on KGI during cold conditions associated with easterly and southerly flows, low melt rates and high lapse rates of nearly 1 K/100 m, whereas during situations of northwest advection of warm, moist air, the melt rates increase concurrent with low and at times positive lapse rates (time period 1997/1998). They give an average lapse rate of 0.58 K/100 m for elevations between 84–255 m a.s.l. and 0.66 K/100 m for elevations between 84–619 m a.s.l. Wen et al. (1994) report a lapse rate of 0.79 K/100 m for austral summer and 0.66 K/100m for winter for elevations below 255 m a.s.l. (time period 1991–1992). Calculating the adiabatic temperature lapse rate Γ between 25 and 230 m a.s.l. from the SMN and AWS datasets (Index SMN) shows an extreme outlier for the winter month June 2011:

$$\overline{\Gamma_{June\ 11,\ SMN}} = -1.02 \pm 1.12\ K/100m$$

with an opposite sign than in 2012:

$$\overline{\Gamma_{June\ 12,\ SMN}} = 0.65 \pm 1.65\ K/100m$$

The monthly mean barometric pressure displays the distinct predominent weather systems. During June 2011, KGI proved to be under strong influence of the Antarctic high pressure system (Fig. 12). June 2012 on the other hand, shows a very low average value, indicating that boundary layer conditions are dominated by cyclonic activities with advection of warm, moist air and an extended melt period (see Fig. 13). The lapse rate analysis for the austral winter month June 2013 is available for the upper ice cap between 230 and 435 m a.s.l. and yields to:

$$\overline{\Gamma_{June,\ up}} = 1.05 \pm 0.62\ K/100m$$

The monthly mean lapse rate shows a high interannual variability and strong dependence on dominating synoptic conditions as well as atmospheric boundary layer conditions. Melt conditions lead to a fixation of the calculated lapse rate at the melting point temperature, inducing a high spatial variability. The exposure to synoptic weather patterns on the upper glacier and a decoupling of the atmospheric surface layer above the upper glacier to the lower coastal areas, contribute to the spatial variability. The surface air temperature lapse rate of the upper transect on the Fourcade Glacier for the austral summer months December to February (2012 to 2013; Fig. 11) averages to

$$\overline{\Gamma_{summer,\ up}} = 0.67 \pm 0.4\ K/100m$$

and for the lower transect of the glacier to

$$\overline{\Gamma_{summer,\ low}} = 0.88 \pm 0.35\ K/100m$$

showing a significant decrease in lapse rate with elevation. Figure 12 also demonstrates the temporal variability and distinct seasonal cycle with significantly higher standard deviations for winter months, with the maximum lapse rate observed in June 2011.

This shows the distinct exposure and higher sensitivity of the upper Warszawa Icefield to synoptic weather patterns and free atmosphere conditions. Gardener et al. (2009) state that the air temperature lapse rate varies on diurnal and seasonal time scales due to changes in sensible heat flux between the free atmosphere and the underlying surface. Near surface lapse rates above melting glaciers are often observed to be lower due to the fixation of melting point temperatures (Greuell and Böhm 1998), and Shawn et al. (2007) find systematically lower than free atmosphere lapse rates measured over Arctic glaciers. Braun and Hock (2004) draw the conclusion that only employment of actual temperature lapse rates can account for the variability in the variable and thus in the accurate ablation estimates for the KGI ice cap. Gardener et al. (2009) conclude under warming climate scenarios, lower lapse rates can be expected.

A quantity strongly related to glacier melt is the positive degree-day (PDD). Calculating the PDD for the AWS site on the Fourcade Glacier from SMN temperature data with standard moist adiabatic temperature lapse rate of free atmosphere of 0.65 K/100m leads to an overestimation of the PDD by a factor of 2.7. Braun and Hock (2004) emphasize the sensitivity of the applied glacier melt model to the applied air temperature lapse rate and name the accurate lapse rate estimation a prerequisite for accuracy of glacier melt model.

5.3 Implications for glacier melt estimates

The analysis carried out in this paper shows that the consequences of the climate change on the study area (KGI) during the past decades include a significant warming of the atmospheric surface layer, increased occurrence of mesocyclones during winter time in the area and changes in the spatio-temporal patterns of the lower tropospheric temperature lapse rate. The detected higher frequency of low-pressure systems hitting KGI during the winter months reveals that the South Shetland Islands are under a progressive increase of melt periods. This fact is in accordance with the findings of Liu et al. (2005) and Liu and Wang (2006) for the north of the AP (melt duration > 90 days per year). Our data show that aside from the prolonged melt period in the austral autumn, significant melt periods also occur during the austral winter with melt rates of as much as 25 cm w.e. per month during the austral winter 2013 (see Fig. 13). Moreover, storm events from cyclonic activity along the winter months enhance the ablation of the snowpack by erosion through precipitation in form of rain. The high spatial variability of surface air temperature across the ice cap of KGI is connected to the high exposure to synoptic influences. This stresses the importance of considering the spatial variability of surface air temperature fields when estimating the glacier surface mass and energy balance of the inland ice cap of the KGI, and in general for the northern Antarctic Peninsula. For KGI, Braun and Hock (2004) give an hourly course for glacier melt rates over a 6-week period in austral summer 1997/1998. The daily maximum hourly value can be up to 4.2 cm w.e./d, comparable to summer melt rates shown in figure 13. The calculated summer mass balance b_s for the AWS location on the Fourcade Glacier for 2010 – 2015 shows persistent negative values for the past years.

The equilibrium line altitude (ELA), i.e., the altitude where ablation equals accumulation is an important glaciological parameter in the context of climate change. In agreement with different authors (e.g., Marshall et al. 1995), the late-summer firn line can be regarded as an approximation of the ELA. Braun (2001) gives 250 m for the ELA position for Fildes Peninsula on KGI, whereas Bintanja (1995) published an ELA position of 150 m for the early 90s. The distinctly negative mass balance estimates for the AWS location on the Fourcade glacier (Tab. 1) clearly show that the ELA is explicitly higher than at an altitude of 230 m.

Only a few studies on glacier melt and mass balance have been carried out for single years or very short time periods on the AP. For example, Schneider (1999) computed surface energy balance components on glaciers in the inner Marguerite Bay, Casassa (1989) for Anver Island, Wager and Jamieson (1983) and Morris (1999) for Alexander Island. Skvarca et al. (2004) presented the first pluriannual glacier mass balance record for "Glaciar Bahía del Diablo" at Vega Island, showing that there is a very strong correlation between annual net mass balance and mean summer air temperatures. However, Morris and Mulvaney (2004) showed that even only integrating very few recent datasets leads to a correction of their previous estimates for the contribution of the AP ice melt to global sea level rise upwards by a factor of almost 2 to 0.007 ±0.02 mm a-1 K-1. The latest estimate for the entire AP glacier melt contribution to sea level rise is given by Vaughan (2006) with 0.008-0.055 mm $a^{-1}K^{-1}$. It has to be considered that these melt estimates are based on very few in-situ observations and/or almost exclusively on datasets recorded at coastal stations. Braun and Hock (2004) showed that for distributed melt modeling on KGI, the consideration of actual often smaller hypsometric air temperature lapse rates are important to reproduce observed ablation rates. As a consequence, the proposed melt estimates given by Vaughan (2006) might be too small as the study is based on station data along the coast and applied a fixed average temperature lapse rate.

Uncertainties in glacier surface mass balance and mass losses are large (e.g., Pritchard and Vaughan 2007; Rignot et al. 2008) and show high spatial variability particularly for the northern part of Antarctica (Turner et al. 1997; van de Berg et al. 2006; Arigony-Neto et al. 2009; Barrand et al. 2013). There are long-term time series of temperature measurements mainly only from coastal stations. The climatological assessments of the atmospheric surface layer that was carried out in this paper show that differences in temperature measurements of an AWS on the inland ice cap to the regular temperature measurements at the coastal Carlini Station are highly variable, especially during austral winters. It was also determined that there are pronounced melt periods driven by high air temperatures and precipitation in form of rain in the winter season.

Acknowledgements

We would like to thank the Alfred Wegener Institute (AWI) from Germany and the Instituto Antártico Argentino - Dirección Nacional del Antártico (IAA-DNA) from Argentina for their support in Antarctica. A special acknowledgement goes to the overwintering scientists at Carlini Station and Dallmann Laboratory: Dr. Damián López, Daniel Viqueira and Juan Piscicelli. During the period 2010–2014, the overwintering crews from the Ejército Argentino at Carlini Station continuously supported our scientific tasks. All photos were taken, processed and provided by the 2012 overwinterer Dr. Damián López, which we are very grateful for. All graphs in this paper were produced using the R programming language (R Core Team 2014)

We also thank the funding support provided by the IMCONet Project (FP7-PEOPLE-2012-IRSES) and the associated institutions at Germany (Univ. of Bonn, Univ. of Erlangen and the BMBF) and Argentina (IAA-DNA).

References

AARI (2014): Arctic and Antarctic Research Institute. St. Petersburg. http://www.aari.nw.ru/index_en.html (Date: 16.12.2014)

Arigony-Neto, J.; Saurer, H.; Simões, J.; Rau, F.; Jaña, R.; Vogt, S. and Gossmann, H. (2009): Spatial and temporal changes in dry-snow line altitude on the Antarctic Peninsula. In: Climate Change 94, 19–33. DOI: 10.1007/s10584-009-9550-1

Barrand, N.; Vaughan, D.; Steiner, N.; Tedesco, M.; Kuipers Munneke, P.; van den Broeke, M. and Hosking J. (2013): Trends in Antarctic Peninsula surface melting conditions from observations and regional climate modeling. In: Journal of Geophysical Research: Earth Surface 118, 315–330. DOI: 10.1029/2012JF002559

Bassford, R.; Siegert, M.; Dowdeswell, J.; Oerlemans, J.; Glazovsky, A. and Macheret, Y. (2006a): Quantifying the mass balance of ice caps on Severnaya Zemlya, Russian High Arctic. I: Climate and mass balance of the Vavilov Ice Cap. In: Arctic, Antarctic, and Alpine Research 38, 1–12. DOI: 10.1657/1523-0430(2006)038[0001:QTMBOI]2.0.CO;2

Bassford, R.; Siegert, M. and Dowdeswell, J. (2006b): Quantifying the mass balance of ice caps on Severnaya Zemlya, Russian High Arctic. II: Modeling the flow of the Vavilov Ice Cap under the present climate. In: Arctic, Antarctic, and Alpine Research 38, 13–20. DOI: 10.1657/1523-0430(2006)038[0013:QTMBOI]2.0.CO;2

Bintanja, R. (1995): The local surface energy balance of the Ecology Glacier, King George Island, Antarctica: measurements and modelling. In: Antarctic Science 7 (3), 315– 325. DOI: 10.1017/s0954102095000435

Braithwaite, R. (1981): On glacier energy balance, ablation, and air temperature. In: Journal of Glaciology 27 (97), 381–391.

Braun, M. (2001): Ablation on the ice cap of King George Island (Antarctica). An approach from field measurements, modelling and remote sensing. PhD thesis. Freiburg. http://www.freidok.uni-freiburg.de/volltexte/223/

Braun, M. and Gossmann, H. (2002): Glacial changes in the areas of Admiralty Bay and Potter Cove, King George Island, Maritime Antarctica. In: Beyer, L. and Bölter, M. (eds.): Geoecology of Antarctic ice-free coastal landscapes. Ecological Studies 154. Berlin, Heidelberg, 75–89. DOI: 10.1007/978-3-642-56318-8_6

Braun, M. and Hock, R. (2004): Spatially distributed surface energy balance and ablation modelling on the ice cap of King George Island (Antarctica). In: Global and Planetary Change 42, 45–58. DOI: 10.1016/j.gloplacha.2003.11.010

Casassa, G. (1989): Velocity, heat budget and mass balance at Anvers Island ice cap, Antarctic Peninsula. In: Antarctic record 33, 341–352.

Cook, A.; Fox, A.; Vaughan, D. and Ferrigno, J. (2005): Retreating glacier fronts on the Antarctic Peninsula over the past half-century. In: Science 308, 541–544. DOI: 10.1126/science.1104235

Cuffey, K. M., and Paterson, W. S. B. (2010): The physics of glaciers. Burlington, MA.

de Woul, M.; Hock, R.; Braun, M.; Thorsteinsson, T.; Jóhannesson, T. and Halldorsdóttir, S. (2006): Firn layer impact on glacial runoff: a case study at Hofsjokull, Iceland. In: Hydrological Processes 20, 2171–2185. DOI: 10.1002/hyp.6201

Falk, U.; Gieseke, H.; Kotzur, F. and Braun, M. (2015): Monitoring snow and ice surfaces on King George Island, Antarctic Peninsula, with high-resolution TerraSAR-X time series. In: Antarctic Science (in press). DOI: 10.1017/S0954102015000577

Ferron, F.; Simões, J. and Aquino, F. (2001): Série temporal de temperatura atmosférica para la Ilha Rei George, Antártica. In: Revista do Departamento de Geografia 14, 25–32.

Gardner, A.; Sharp, M.; Koerner, R.; Labine, C.; Boon, S.; Marshall, S.; Burgess, D. and Lewis, D. (2009: Near-surface temperature lapse rates over Arctic glaciers and their implications for temperature downscaling. In: Journal of Climate 22, 4281–4298. DOI: 10.1175/2009JCLI2845.1

Gillett, N.; Kell, T. and Jones, P. (2006): Regional climate impacts of the Southern Annular Mode. In: Geophysical Research Letters 33, L23704. DOI: 10.1029/2006GL027721

Glover, R. (1999): Influence of spatial resolution and treatment of orography on GCM estimates of the surface mass balance of the Greenland Ice Sheet. In: Journal of Climate 12, 551–563. DOI: 10.1175/1520-0442(1999)012<0551:IOSRAT>2.0.CO;2

Gong, D. and Wang, S. (1999): Definition of Antarctic oscillation index. In: Geophysical Research Letters 26, 459–462. DOI: 10.1029/1999GL900003

Greuell, W. and Böhm, R. (1998): 2 m temperatures along melting mid-latitude glaciers, and implications for the sensitivity of the mass balance to variations in temperature. In: Journal of Glaciology 44 (146), 9–20.

Hock, R. (2003): Temperature index melt modelling in mountain areas. In: Journal of Hydrology 282, 104–115. DOI: 10.1016/S0022-1694(03)00257-9

Hock, R; de Woul, M.; Radic, V. and Dyurgerov, M. (2009): Mountain glaciers and ice caps around Antarctica make a large sea-level rise contribution. In: Geophysical Research Letters 36, L07501. DOI: 10.1029/2008GL037020

IPCC (2013): Climate Change 2013: The Physical Science Basis. Contribution of Working Group I to the Fifth Assessment Report of the Intergovernmental Panel on Climate Change [Stocker, T.; Qin, D.; Plattner, G-K.; Tignor, M.; Allen, S.; Boschung, J.; Nauels, A.; Xia, Y.; Bex, V. and Midgley, P. (eds.)]. Cambridge, U. K., New York.

Kalnay, E.; Kanamitsu, M.; Kistler, R.; Collins, W.; Deaven, D.; Gandin, L.; Iredell, M.; Saha, S.; White, G.; Woollen, J.; Zhu, Y.; Leetmaa, A. and Reynolds, R. (1996): The NCEP/NCAR 40-Year Reanalysis Project. In: Bulletin of the American Meteorological Society 77, 437–471. DOI: 10.1175/1520-0477(1996)077<0437:tnyrp>2.0.co;2

Liu, H. and Wang, L. (2006): Spatiotemporal variations of snowmelt in Antarctica derived from satellite scanning multichannel microwave radiometer and Special Sensor Microwave Imager data (1978–2004). In: Journal of Geophysical Research 111, F01003. DOI: 10.1029/2005JF000318

Liu, H.; Wang, L. and Jezek, K. (2005): Wavelet-transform based edge detection approach to derivation of snowmelt onset, end and duration from satellite passive microwave measurements. In: International Journal of Remote Sensing 26, 4639–4660. DOI: 10.1080/01431160500213342

Lubin, D.; Wittenmyer, R.; Bromwich, D. and Marshall, G. (2008): Antarctic Peninsula mesoscale cyclone variability and climatic impacts influenced by the SAM. In: Geophysical Research Letters 35, L02808. DOI: 10.1029/2007GL032170

Marshall, G. J. (2003): Trends in the Southern Annular Mode from observations and reanalyses. In: Journal of Climate 16, 4134–4143. DOI: 10.1175/1520-0442(2003)016<4134:TITSAM>2.0.CO;2

– (2009): On the annual and semi-annual cycles of precipitation across Antarctica. In: International Journal of Climatology, 29, 2298–2308. DOI: 10.1002/joc.1810

Marshall, G. J.; Rees, W. G. and Dowdeswell, J. A. (1995): The discrimination of glacier facies using multi-temporal ERS-1 SAR data. In Askne, J. (ed.): Sensors and environmental applications of remote sensing. Rotterdam, 263–269.

Martianov, V. and Rakusa-Suszczewski, S. (1989): Ten years of climate observations at the Arctowski and Bellingshausen stations (King George Is., South Shetlands, Antarctica). In: Breymeyer, A. (ed.): Global change regional research centres: scientific problems and concept developments. Seminar papers and IGBP WG 2 Report, 80–87. Warszawa.

Meredith, M. and King, J. (2005): Rapid climate change in the ocean west of the Antarctic Peninsula during the second half of the 20th century. In: Geophysical Research Letters, 32, L19604. DOI: 10.1029/2005GL024042

Morris, E. (1999): Surface ablation rates on Moraine Corrie Glacier, Antarctica. In: Global and Planetary Change 22, 221–231. DOI: 10.1016/s0921-8181(99)00039-9

Morris, E. and Mulvaney, R. (2004): Recent variations in surface mass balance of the Antarctic Peninsula ice sheet. In: Journal of Glaciology 50, 257–267. DOI: 10.3189/172756504781830051

Nan, S. and Li, J. (2003): The relationship between the summer precipitation in the Yangtze River valley and the boreal spring Southern Hemisphere annular mode. In: Geophysical Research Letters 30 (24), 2266. DOI: 10.1029/2003GL018381

NOAA (1976): U.S. Standard Atmosphere, 1976. Washington, DC.

Parish, T. and Bromwich, D. (2007): Reexamination of the near-surface airflow over the Antarctic continent and implications on atmospheric circulations at high southern latitudes. In: Monthly Weather Review 135, 1961–1973. DOI: 10.1175/MWR3374.1

Park, B.; Park, B.; Chang, S.; Yoon, H. and Chung, H. (1998): Recent retreat of the ice cliffs on King George Island, South Shetland Islands, Antarctic Peninsula. In: Annals of Glaciology 27, 633–635.

Pritchard, H. and Vaughan, D. (2007): Widespread acceleration of tidewater glaciers on the Antarctic Peninsula. In: Journal of Geophysical Research 112, F03S29. DOI: 10.1029/2006JF000597

Raper, S. and Braithwaite, R. (2006): Low sea level rise projections from mountain glaciers and icecaps under global warming. In: Nature 439, 311–313. DOI: 10.1038/nature04448

Rau, F. and Braun, M. (2002): The regional distribution of the dry-snow zone on the Antarctic Peninsula north of 70°S. In: Annals of Glaciology 34, 95–100. DOI: 10.3189/172756402781817914

Rignot, E. (2008): Changes in West Antarctic ice stream dynamics observed with ALOS PALSAR data. In: Geophysical Research Letters 35, L12505. DOI: 10.1029/2008GL033365

Rignot, E.; Bamber, J.; van den Broeke, M.; Davis, C.; Yonghong, L.; van de Berg, W.; van Meijgaard, E. (2008): Recent Antarctic ice mass loss from radar interferometry and regional climate modelling. In: Nature Geoscience 1, 106–110. DOI: 10.1038/ngeo102

Rückamp, M.; Braun, M.; Suckro, S. and Blindow, N. (2011): Observed glacial changes on the King George Island ice cap, Antarctica, in the last decade. In: Global and Planetary Change 79, 99–109. DOI: 10.1016/j.gloplacha.2011.06.009

Sala, H.; Matko, C.; Falk, U. and Grings, F. (2014): Análisis y comparación de dos modelos digitales de elevación en la Isla 25 de Mayo (King George Island), Islas Shetland del Sur, Antártida. In: Geoacta 39, 14–29.

Schneider, C. (1999): Energy balance estimates during the summer season of glaciers of the Antarctic Peninsula. In: Global and Planetary Change 22, 117–130. DOI: 10.1016/S0921-8181(99)00030-2

Shawn, J.; Sharp, M.; Burgess, D. and Anslow, F. (2006): Near-surface-temperature lapse rates on the Prince of Wales Icefield, Ellesmere Island, Canada: implications for regional downscaling of temperature. In: International Journal of Climatology 27 (3), 385–398. DOI: 10.1002/joc.1396

Shindell, D. and Schmidt, G. (2004): Southern Hemisphere climate response to ozone changes and greenhouse gas increases. In: Geophysical Research Letters 31, L18209. DOI: 10.1029/2004GL020724

Simões, J.; Bremer, U.; Aquino, F. and Ferron, F. (1999): Morphology and variations of glacial drainage basins in the King George Island ice field, Antarctica. In: Annals of Glaciology 29, 220–224. DOI: 10.3189/172756499781821085

Singh, V. P.; Singh, P. and Haritashya, U. K. (eds.) (2011): Encyclopedia of snow, ice and glaciers. Dordrecht. DOI: 10.1007/978-90-481-2642-2

Skvarca, P.; De Angelis, H. and Ermolin, E. (2004): Mass balance of 'Glaciar Bahía del Diablo', Vega Island, Antarctic Peninsula. In: Annals of Glaciology 39, 209–213. DOI: 10.3189/172756404781814672

Skvarca, P.; Rack, W.; Rott, H. and Ibarzábal y Donángelo, T. (1999): Climatic trend and the retreat and disintegration of ice shelves on the Antarctic Peninsula: an overview. In: Polar Research 18, 151–157. DOI: 10.1111/j.1751-8369.1999.tb00287.x

Smith, R. and Stammerjohn, S. (2001): Variations of surface air temperature and sea-ice extent in the western Antarctic Peninsula region. In: Annals of Glaciology 33 (1), 493–500. DOI: 10.3189/172756401781818662

SMN (2013): Servicio Meteorológico Nacional, Argentina. http://www.smn.gov.ar/ (Date: 12.12.2014)

Solomon, S.; Plattner, G-K.; Knutti, R. and Friedlingstein, P. (2009). Irreversible climate change due to carbon dioxide emissions. In: Proceedings of the National Academy of Sciences of the United States of America 106 (6), 1704–1709. DOI: 10.1073/pnas.0812721106

Tedesco, M. and Monaghan, A. (2009): An updated Antarctic melt record through 2009 and its linkages to high-latitude and tropical climate variability. In: Geophysical Research Letters 36, L18502. DOI: 10.1029/2009GL039186

Thompson, D. and Solomon, S. (2002): Interpretation of recent Southern Hemisphere climate change. In: Science 296, 895–899. DOI: 10.1126/science.1069270

Torinesi, O.; Fily, M. and Genthon, C. (2003): Variability and trends of the summer melt period of Antarctic ice margins since 1980 from microwave sensors. In: Journal of Climate 16, 1047–1060. DOI: 10.1175/1520-0442(2003)016<1047:VATOTS>2.0.CO;2

Thomas, R. H.; Abdalati, W. W.; Frederick, E.; Krabill, W. B.; Manizade, S. and Steffen, K. (2003): Investigation of surface melting and dynamic thinning on Jakobshan Isbrae, Greenland. In: Journal of Glaciology 49, 231–239. DOI: 10.3189/172756503781830764

Trusel, L.; Frey, K. and Das, S. (2012): Antarctic surface melting dynamics: enhanced perspectives from radar scatterometer data. In: Journal of Geophysical Research 117, F02023. DOI: 10.1029/2011JF002126

Turner, J. (2004): The El Niño-southern oscillation and Antarctica. In: International Journal of Climatology 24, 1–31. DOI: 10.1002/joc.965

Turner, J.; Colwell, S. and Harangozo, S. (1997): Variability of precipitation over the coastal western Antarctic Peninsula from synoptic observations. In: Journal of Geophysical Research 102, 13999–14007. DOI: 10.1029/96JD03359

Turner, J.; Colwell, S.; Marshall, G.; Lachlan-Cope, T.; Carleton, A.; Jones, P.; Lagun, V.; Reid, P. and Iagovkina, S. (2004): The SCAR READER project: toward a high-quality database of mean Antarctic meteorological observations. In: Journal of Climate 17, 2890–2898. DOI: 10.1175/1520-0442(2004)017<2890:TSRPTA>2.0.CO;2

van de Berg, W.; van den Broeke, M.; Reijmer, C. and van Meijgaard, E. (2006): Reassessment of the Antarctic surface mass balance using calibrated output of a regional atmospheric climate model. In: Journal of Geophysical Research 111, D11. DOI: 10.1029/2005JD006495

van den Broeke, M. (2000): On the interpretation of Antarctic temperature trends. In: Journal of Climate 13, 3885–3889. DOI: 10.1175/1520-0442(2000)013<3885:OTIOAT>2.0.CO;2

van den Broeke, M.; van de Berg, W. and van Meijgaard, E. (2006): Snowfall in coastal West Antarctica much greater than previously assumed. In: Geophysical Research Letters 33, L02505. DOI: 10.1029/2005GL025239

van Loon, H. (1967): The half-yearly oscillations in the middle and high southern latitudes and the coreless winter. In: Journal of the Atmospheric Sciences 24, 472–486. DOI: 10.1175/1520-0469(1967)024<0472:THYOIM>2.0.CO;2

Vaughan, D.; Marshall, G.; Connolley, W.; Parkinson, C.; Mulvaney, R.; Hodgson, D.; King, J.; Pudsey, C. and Turner, J. (2003): Recent rapid regional climate warming on the Antarctic Peninsula. In: Climate Change 60, 243–274. DOI: 10.1023/A:1026021217991

Vaughan, D. (2006): Recent trends in melting conditions on the Antarctic Peninsula and their implications for ice-sheet mass balance and sea level. In: Arctic, Antarctic and Alpine Research 38, 147–152. DOI: 10.1657/1523-0430(2006)038[0147:rtimco]2.0.co;2

Wager, A. and Jamieson, A. (1983): Glaciological characteristics of Spartan Glacier, Alexander Island. In: British Antarctic Survey Bulletin 52, 221–228.

Wen, J.; Kang, J.; Han, J.; Xie, Z.; Liu, L. and Wang, D. (1998): Glaciological studies on King George Island ice cap, South Shetland Islands, Antarctica. In: Annals of Glaciology 27, 105–109.

Zazulie, N.; Rusticucci, M. and Solomon, S. (2010): Changes in climate at high southern latitudes: a unique daily record at Orcadas spanning 1903–2008. In: Journal of Climatology 23, 189–196. DOI: 01175/2009JCLI3074.1

Authors

Dr. Ulrike Falk
University of Bonn
Center for Remote Sensing of Land Surfaces (ZFL)
Walter-Flex-Strasse 3
53113 Bonn
Germany
ulrike.falk@gmail.com

Lic. Hernán Sala
Instituto Antártico Argentino
Dirección Nacional del Antártico
Balcarce 290 - 2° Piso, C.A.B.A. C1064ABR
Buenos Aires
Argentina
hersala@gmail.com